BLACK HOLE–NEUTRON STAR MERGERS AS CENTRAL ENGINES OF GAMMA-RAY BURSTS

H.-Thomas Janka,[1] Thomas Eberl,[1,2] Maximilian Ruffert,[3] and Chris L. Fryer[4]

ABSTRACT

Hydrodynamic simulations of the merger of stellar mass black hole–neutron star binaries are compared with mergers of binary neutron stars. The simulations are Newtonian but take into account the emission and back-reaction of gravitational waves. The use of a physical nuclear equation of state allows us to include the effects of neutrino emission. For low neutron star–to–black hole mass ratios, the neutron star transfers mass to the black hole during a few cycles of orbital decay and subsequent widening before finally being disrupted, whereas for ratios near unity the neutron star is destroyed during its first approach. A gas mass between ~0.3 and ~0.7 $M_\odot$ is left in an accretion torus around the black hole and radiates neutrinos at a luminosity of several times 10^{53} ergs s^{-1} during an estimated accretion timescale of about 0.1 s. The emitted neutrinos and antineutrinos annihilate into $e^\pm$ pairs with efficiencies of 1%–3% and rates of up to ~2×10^{52} ergs s^{-1}, thus depositing an energy $E_{\nu\bar\nu} \lesssim 10^{51}$ ergs above the poles of the black hole in a region that contains less than 10^{-5} $M_\odot$ of baryonic matter. This could allow for relativistic expansion with Lorentz factors around 100 and is sufficient to explain apparent burst luminosities $L_\gamma \sim E_{\nu\bar\nu}/(f_\Omega t_\gamma)$ up to several times 10^{53} ergs s^{-1} for burst durations $t_\gamma \approx 0.1$–1 s, if the γ emission is collimated in two moderately focused jets in a fraction $f_\Omega = 2\delta\Omega/(4\pi) \approx (1/100)$–$(1/10)$ of the sky.

Subject headings: binaries: close — black hole physics — gamma rays: bursts — stars: neutron

1. INTRODUCTION

Black hole–neutron star binary (BH/NS) and binary neutron star (NS/NS) mergers are thought to be promising candidates for the origin of gamma-ray bursts (GRBs; e.g., Blinnikov et al. 1984; Eichler et al. 1989; Paczyński 1991; Narayan, Piran, & Shemi 1991; Mészáros 1999; Fryer, Woosley, & Hartmann 1999; Bethe & Brown 1998, 1999), at least for the subclass of less complex and less energetic short and hard bursts (Mao, Narayan, & Piran 1994) with durations of fractions of a second (Popham, Woosley, & Fryer 1999; Ruffert & Janka 1999). Optical counterparts and afterglows of this subclass have not yet been observed. Because of the presence of a region of very low baryon density above the poles of the black hole, BH/NS mergers are considered to be more favorable sources than NS/NS mergers (e.g., Portegies Zwart 1998; Brown et al. 1999).

Previous Newtonian smoothed particle hydrodynamic simulations of BH/NS mergers using a polytropic equation of state indicate that the neutron star may slowly lose gas in many mass transfer cycles (Kluźniak & Lee 1998; Lee & Kluźniak 1998, 1999). Whether dynamical instability sets in at a minimum separation (Rasio & Shapiro 1994; Lai, Rasio, & Shapiro 1994) or whether stable Roche lobe overflow takes place, however, can depend on the neutron star–to–black hole mass ratio (Bildsten & Cutler 1992) and the properties of the nuclear equation of state, expressed by the adiabatic index (Uryū & Eriguchi 1999).

In this Letter, we report on the first Newtonian BH/NS merger simulations (Eberl 1998), which were done with a realistic nuclear equation of state (Lattimer & Swesty 1991) and which therefore yield information about thermodynamic evolution and neutrino emission. They allow one to compare the strength of the gravitational wave (GW) emission relative to NS/NS mergers and to investigate neutrino-antineutrino ($\nu\bar\nu$) annihilation as a potential source of energy for GRBs.

2. NUMERICAL METHODS

The three-dimensional hydrodynamic simulations were performed with a Eulerian piecewise parabolic method code using four levels of nested Cartesian grids, which ensure good resolution near the center of mass and a large computational volume simultaneously. Each grid had 64^3 zones; the size of the smallest zone was 0.64 or 0.78 km in case of NS/NS and 1.25 or 1.5 km for BH/NS mergers. The zone sizes of the next coarser grid levels were doubled to cover a volume of 328 or 400 km side length for NS/NS and 640 or 768 km for BH/NS simulations. GW emission and its back-reaction on the hydrodynamics were taken into account by the method of Blanchet, Damour, & Schäfer (1990; see also Ruffert, Janka, & Schäfer 1996). The neutrino emission and corresponding energy and lepton number changes of the matter were calculated with an elaborate neutrino leakage scheme (Ruffert et al. 1996), and $\nu\bar\nu$ annihilation around the merger was evaluated in a postprocessing step (Ruffert et al. 1997).

3. SIMULATIONS

Table 1 gives a list of computed NS/NS and BH/NS merger models. Besides the baryonic mass of the neutron star and the mass of the black hole, the spins of the neutron stars were varied. The cool neutron stars have a radius of about 15 km (Ruffert et al. 1996), and the runs were started with a center-to-center distance of 42–46 km for NS/NS's and with 47 km in case of BH/NS's for $M_{BH} = 2.5$ $M_\odot$, 57 km for $M_{BH} = 5$ $M_\odot$, and 72 km for $M_{BH} = 10$ $M_\odot$. The simulations were stopped at a time t_{sim} between 10 and 20 ms. The black hole was treated as a point mass at the center of a sphere with radius $R_s = 2GM_{BH}/c^2$, which gas could enter unhindered. Its mass and momentum were updated along with the accretion of matter. Model TN10, which is added for comparison, is a continuation of the NS/NS merger model B64 where at time $t_{sim} =$

[1] Max-Planck-Institut für Astrophysik, Postfach 1523, D-85748 Garching, Germany; thj@mpa-garching.mpg.de.
[2] Technische Universität München, Physik-Department E12, James-Franck-Strasse, D-85748 Garching, Germany; thomas.eberl@physik.tu-muenchen.de.
[3] Department of Mathematics and Statistics, University of Edinburgh, EH9 3JZ, Scotland, UK; m.ruffert@ed.ac.uk.
[4] UCO/Lick Observatory, University of California, Santa Cruz, Santa Cruz, CA 95064; cfryer@ucolick.org.

TABLE 1
GRAVITY WAVES AND NEUTRINOS FROM NS/NS AND BH/NS MERGING

Model	Masses ($M_\odot$)	Spin	t_{sim} (ms)	L_{GW}^{max} (10^4 foe s^{-1})[a]	rh^{max} (10^4 cm)	E_{GW} (foe)	$L_{\nu_e}^{max(av)}$ (100 foe s^{-1})	$L_{\bar{\nu}_e}^{max(av)}$ (100 foe s^{-1})	$L_{\Sigma\nu_x}^{max(av)}$ (100 foe s^{-1})	E_ν (foe)	kT^{max} (MeV)	$\langle\epsilon_{\nu_e}\rangle$ (MeV)	$\langle\epsilon_{\bar{\nu}_e}\rangle$ (MeV)	$\langle\epsilon_{\nu_x}\rangle$ (MeV)
						NS/NS								
S64	1.2+1.2	Solid	10	0.7	5.5	14	0.3(0.2)	0.9(0.5)	0.3(0.2)	0.8	35	12	18	26
D64	1.2+1.8	Solid	13	0.4	5.5	13	0.5(0.3)	1.3(0.8)	0.7(0.4)	1.1	35	13	19	27
V64	1.6+1.6	Anti	10	1.2	6.0	23	1.1(0.5)	2.6(1.3)	0.7(0.3)	1.9	69	13	19	27
A64	1.6+1.6	None	10	2.1	8.6	52	0.9(0.5)	2.6(1.3)	1.4(0.6)	2.3	39	12	18	26
B64	1.6+1.6	Solid	10	2.1	8.9	37	0.6(0.4)	1.8(1.1)	0.9(0.4)	1.8	39	13	19	27
						BH/AD								
TN10	2.9+0.26	Solid	15	...	...	...	0.5(0.4)	1.3(0.9)	0.6(0.2)	0.8	15	9	13	21
						BH/NS								
C2.5	2.5+1.6	Anti	10	2.3	9.9	32	1.5(0.5)	7.3(2.5)	5.2(1.9)	4.5	74	16	22	31
A2.5	2.5+1.6	None	10	2.0	9.9	50	1.8(0.5)	6.4(2.2)	3.1(1.3)	3.6	65	15	22	31
B2.5	2.5+1.6	Solid	10	2.1	9.6	61	0.9(0.3)	6.5(1.7)	3.6(0.9)	2.5	61	14	21	29
C5	5.0+1.6	Anti	15	3.9	13.0	50	0.7(0.4)	3.8(1.6)	2.5(1.1)	4.5	46	15	20	29
A5	5.0+1.6	None	20	3.2	14.8	102	0.7(0.2)	4.4(1.5)	2.8(0.8)	4.5	51	16	24	31
B5	5.0+1.6	Solid	15	3.4	14.5	95	0.6(0.2)	3.7(1.1)	2.5(0.6)	2.9	44	14	21	28
C10	10.0+1.6	Anti	10	7.1	21.9	123	0.4(0.1)	2.5(0.4)	1.2(0.1)	0.6	51	14	19	24
A10	10.0+1.6	None	10	6.9	26.2	168	0.2(0.1)	2.5(0.5)	1.2(0.2)	0.7	50	14	20	26
B10	10.0+1.6	Solid	10	7.3	26.2	163	0.4(0.1)	2.5(0.8)	1.4(0.2)	1.1	52	13	18	24

NOTE.—"Solid" means synchronously rotating stars, "none" denotes irrotational cases, and "anti" is for counterrotation, i.e., spin vectors opposite to the direction of the orbital angular momentum.

[a] 1 foe = 10^{51} ergs.

10 ms the formation of a black hole was assumed and the accretion was followed for another 5 ms until a steady state was reached (Ruffert & Janka 1999).

4. RESULTS

4.1. *Evolution of BH/NS Mergers*

Because of the emission of GWs, the orbital separation decreases. During its first approach, the neutron star transfers matter to the black hole at huge rates of several hundred up to ~1000 $M_\odot$ s^{-1}. Within 2–3 ms it loses 50%–75% of its initial mass. In case of the 2.5 $M_\odot$ black hole, the evolution is catastrophic and the neutron star is immediately disrupted (Lattimer & Schramm 1974). A mass of 0.2–0.3 $M_\odot$ remains in a thick disk around the black hole (M_d in Table 2). In contrast, the orbital distance increases again for $M_{BH} = 5$ and 10 $M_\odot$ and a significantly less massive neutron star begins a second approach. Again, the black hole swallows gas at rates of more than 100 $M_\odot$ s^{-1}. Even a third cycle is possible (Fig. 1). Finally,

at a distance d_{ns} and time t_{ns}, the neutron star with a mass of M_{ns}^{min} is destroyed and most of its mass ends up in an accretion disk (Table 2). (In case of NS/NS mergers, t_{ns} means the time when the two density maxima of the stars are one stellar radius, i.e., $d_{ns} = 15$ km, apart.)

The increase of the orbital separation is connected with a strong rise of the specific (orbital) angular momentum of the gas (Fig. 1). Partly this is due to the fact that the black hole can capture gas with low specific angular momentum first, but mainly it is because only a fraction of the orbital angular momentum of the accreted gas is fed into spinning up the black hole. This fraction, which is lost for the orbital motion, is proportional to the quantity α in Figure 2. Figure 2 is based on the parameterized analysis of nonconservative mass transfer by Podsiadlowski, Joss, & Hsu (1992; see also Fryer et al. 1999) assuming that mass ejection from the system is negligible. It shows that disregarding GW emission, the orbital separation can increase for small initial black hole mass only after the neutron star has lost much mass, while for larger initial

TABLE 2
DISK FORMATION AND NEUTRINO ANNIHILATION

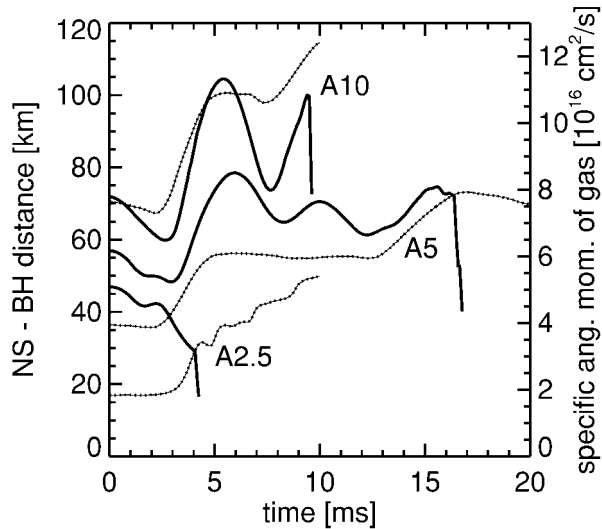| Model	t_{ns} (ms)	d_{ns} (km)	M_{ns}^{min} ($M_\odot$)	ΔM_{ej} ($M_\odot$/100)	M_d ($M_\odot$)	$\dot{M}_d$ ($M_\odot$ s^{-1})	t_{acc} (ms)	α_{eff} ($\times 10^{-3}$)	a_i	a_f	a_{BH}^∞	$\langle L_\nu\rangle$ (100 foe s^{-1})[a]	$\dot{E}_{\nu\bar{\nu}}$ (foe s^{-1})	q_ν (%)	$q_{\nu\bar{\nu}}$ (%)	E_ν (foe)	$E_{\nu\bar{\nu}}$ (foe)
S64	2.8	15	...	2.0	...	...	...	...	0.98	0.75	...	1.5	1	...	1	...	...
D64	7.3	15	...	3.8	...	...	...	...	0.87	0.69	...	2	2	...	1	...	...
V64	3.7	15	...	0.0085	...	...	...	...	0.64	0.49	...	4	9	...	2	...	...
A64	1.7	15	...	0.23	...	...	...	...	0.76	0.55	...	5	9	...	2	...	...
B64	1.6	15	...	2.4	...	...	...	...	0.88	0.63	...	3	7	...	2	...	...
TN10	...	...	...	...	0.26	5	53	4	...	0.42	0.59	1.2	0.5	1.3	0.4	7	0.03
C2.5	2.6	11	0.78	0.01	0.26	6	43	4	0.65	0.47	0.60	7	20	6	3	30	0.9
A2.5	4.3	18	0.78	0.03	0.33	<14	>24	<8	0.67	0.39	0.56	7	20	>3	3	>17	>0.5
B2.5	6.0	23	0.78	0.2	0.45	<35	>13	<14	0.69	0.38	0.61	7	20	>1	3	>9	>0.3
C5	9.1	76	0.40	2.5	0.38	5	76	5	0.44	0.27	0.42	4	8	4	2	30	0.6
A5	16.3	65	0.52	2.5	0.49	6	82	4	0.45	0.17	0.37	4	8	4	2	33	0.7
B5	10.8	79	0.50	5.6	0.45	6	75	5	0.46	0.19	0.38	4	8	4	2	30	0.6
C10	8.0	96	0.65	2.2	0.67	<10	>67	<11	0.24	0.07	0.25	2	2	>1	1	>13	>0.1
A10	9.3	95	0.60	3.2	0.56	<60	>9	<82	0.25	0.07	0.22	2	2	>0.2	1	>2	>0.02
B10	5.1	97	0.65	10.0	0.47	3	160	5	0.25	0.11	0.23	2	2	4	1	32	0.3

[a] 1 foe = 10^{51} ergs.

FIG. 1.—Orbital separation between black hole and neutron star (*solid lines*) and specific angular momentum of the gas on the grid (*dotted lines*) as functions of time for models A2.5, A5, and A10. The steep drop at the end of the solid lines marks the moment at which the neutron star is disrupted.

M_{BH} and smaller α orbital widening is easier. Without GWs the separation increases when $\alpha < (M_{BH} - M_{NS})/(M_{BH} + M_{NS})$. Including angular momentum loss by GWs in the point-mass approximation and using the mass-loss rates from the hydrodynamic models (*dashed lines*, Fig. 2) yields a qualitative understanding of the behavior visible in Figure 1 and suggests that α is between 0.2 and 0.5.

During the merging a gas mass ΔM_{ej} of $\sim 10^{-4} M_\odot$ (in case of counterrotation and $M_{BH} = 2.5 M_\odot$) to $\sim 0.1 M_\odot$ (corotation and $M_{BH} = 10 M_\odot$) is dynamically ejected (Table 2). In the latter case the associated angular momentum loss is about 7%; in all other cases, it is less than 5% of the total initial angular momentum of the system. Another fraction of up to 24% of the initial angular momentum is carried away by GWs. In Table 2 the rotation parameter $a = Jc/(GM^2)$ is given for the initial state of the binary system (a_i) and at the end of the simulation (a_f) for the remnant of NS/NS mergers or for the black hole in BH/NS systems, respectively, provided the black hole did not have any initial spin. When the whole disk mass M_d has been swallowed by the Kerr black hole, a final value a_{BH}^∞ (Table 2) will be reached in case of the accretion of a corotating, thin disk with maximum radiation efficiency.

The phase of largest mass flow rate to the black hole (between 2 and 5 ms after the start of the simulations) is connected with a maximum of the GW luminosity L_{GW} which reaches up to 7×10^{55} ergs s^{-1} (Table 1). The peak values of L_{GW} and the wave amplitude rh (for distance r from the source) increase with the black hole mass. The total energy E_{GW} radiated in GWs can be as much as $0.1 M_\odot c^2$ for $M_{BH} = 10 M_\odot$.

4.2. Neutrino Emission and GRBs

Compressional heating, shear due to numerical viscosity, and dissipation in shocks heat the gas during accretion to maximum temperatures kT^{max} of several 10 MeV. Average temperatures are between 5 and 20 MeV, the higher values being for the less massive and more compact black holes. At these temperatures and at densities of 10^{10}–10^{13} g cm^{-3} in the accretion flow, electrons are nondegenerate and positrons are abundant. Electron neutrinos and antineutrinos are therefore copiously created
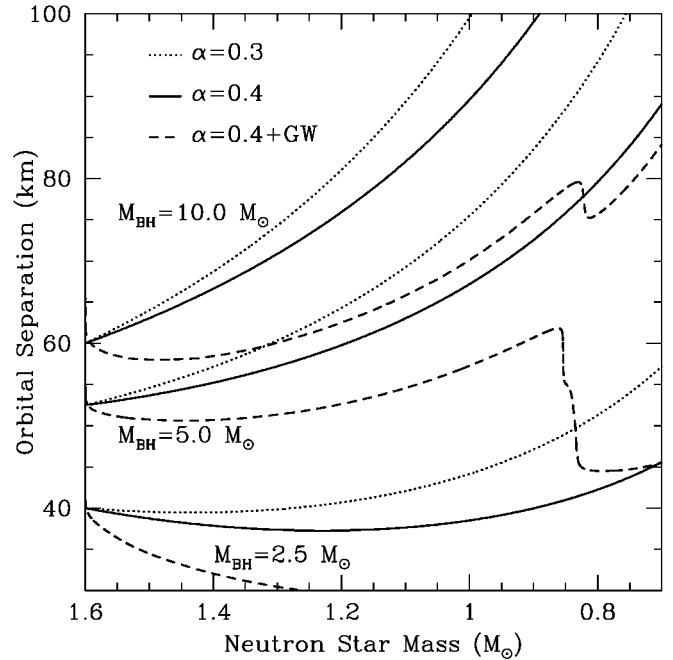

FIG. 2.—Orbital separation as function of neutron star mass for different initial black hole masses and values of parameter α in a simple analytic model (see text). Note that the total mass of the system, $M_{BH} + M_{NS}$ is constant along the lines. Mass transfer leads to orbit widening only for $M_{BH} = 5$ and $10 M_\odot$, whereas GW emission decreases the separation. Combining both effects (*dashed lines*) qualitatively explains the behavior shown for the hydrodynamic simulations in Fig. 1.

via reactions $p + e^- \rightarrow n + \nu_e$ and $n + e^+ \rightarrow p + \bar{\nu}_e$ and dominate the neutrino energy loss from the accreted matter. Dense and hot neutron matter is not completely transparent to neutrinos. By taking into account the finite diffusion time, the neutrino trapping scheme limits the loss of energy and lepton number.

In Table 1 maximum and average values of the luminosities ($L_{\nu_i}^{max}$ and $L_{\nu_i}^{av}$, respectively, the latter in brackets) in the simulated time intervals are listed for ν_e and $\bar{\nu}_e$ and for the sum of all heavy-lepton neutrinos. The latter are denoted by $\nu_x \equiv$
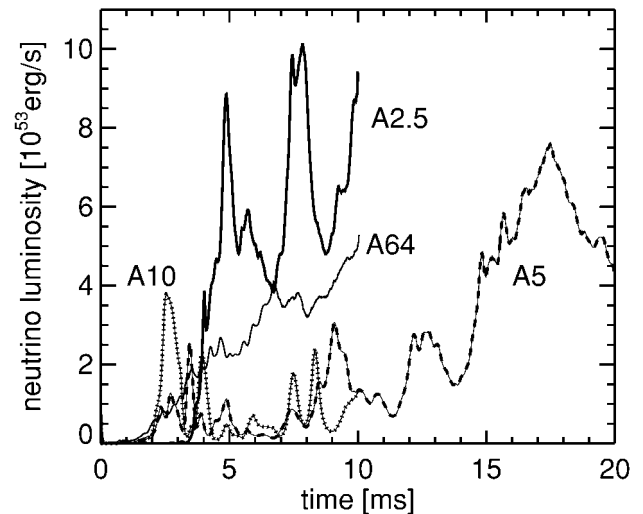

FIG. 3.—Total neutrino luminosities as functions of time for BH/NS merger models A2.5, A5, and A10, and for the NS/NS merger model A64.
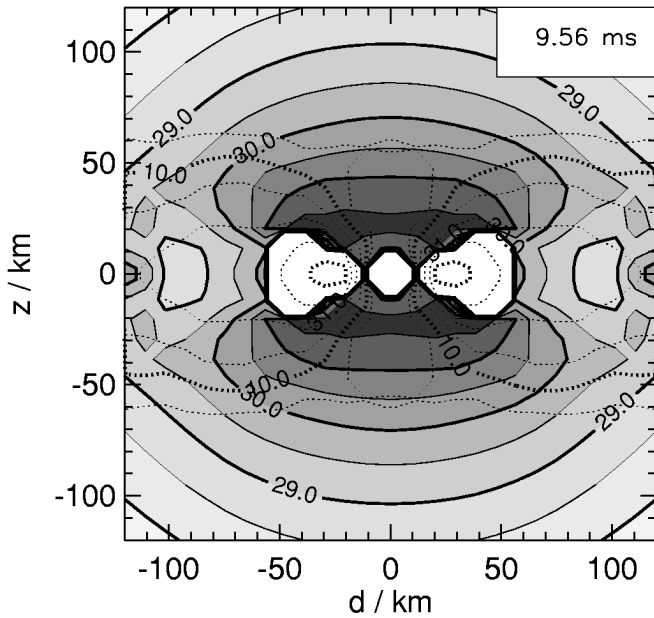
FIG. 4.—Contours of the logarithm of the azimuthally averaged density distribution (*dotted lines*) of the accretion torus around the black hole (*white octagonal area*) and of the logarithm of the energy deposition rate per cm^3 by $\nu\bar{\nu}$ annihilation into e^+e^- pairs (*solid lines*) for the BH/NS merger model C2.5 at time 9.56 ms. The contours are spaced in steps of 0.5 dex. The integral energy deposition rate is 2×10^{52} ergs s^{-1}.

ν_μ, $\bar{\nu}_\mu$, ν_τ, $\bar{\nu}_\tau$ and are mainly produced by e^+e^- annihilation. The total neutrino luminosities $L_\nu(t)$ (Fig. 3) fluctuate strongly with the varying mass transfer rate to the black hole during the cycles of orbital decay and widening (compare with Fig. 1). The total energy E_ν radiated in neutrinos in 10–20 ms is typically several 10^{51} ergs. Time averages of the mean energies $\langle\epsilon\rangle$ of the emitted neutrinos are ~15 MeV for ν_e, 20 MeV for $\bar{\nu}_e$, and 30 MeV for ν_x. Luminosities as well as mean energies, in particular for smaller black holes, are significantly higher than in case of NS/NS mergers.

At the end of the simulations, several of the BH/NS models have reached a steady state, characterized by only a slow growth of the black hole mass with a nearly constant accretion rate. Corresponding rates $\dot{M}_d$ are given in Table 2 and are several $M_\odot$ s^{-1}. From these we estimate torus life times $t_{acc} = M_d/\dot{M}_d$

of 50–150 ms. Values with greater than and less than symbols indicate cases in which the evolution and emission are still strongly time dependent at t_{sim}. In these cases, the accretion torus around the black hole has also not yet developed axial symmetry. In all other cases the effective disk viscosity parameter $\alpha_{eff} \sim v_r/v_{Kepler} \sim 3\sqrt{6}R_S/(t_{acc}c)$, evaluated at a representative disk radius of $3R_S = 6GM_{BH}/c^2$, has the same value, $(4–5) \times 10^{-3}$. This value is associated with the numerical viscosity of the hydrodynamic code (which solves the Euler equations) for the chosen resolution. The further disk evolution is driven by the angular momentum transport mediated by viscous shear forces, which determines the accretion rate. The physical value of the disk viscosity is unknown. The numerical viscosity of our code, however, is in the range in which the viscous energy dissipation and the energy emission by neutrinos should be roughly equal, i.e., where the conversion efficiency $q_\nu = \langle L_\nu\rangle/(\dot{M}_d c^2)$ of rest-mass energy to neutrinos is nearly maximal (see Ruffert et al. 1997; Ruffert & Janka 1999).

Assuming that the average neutrino luminosity $\langle L_\nu\rangle$ at t_{sim} is representative for the subsequent accretion phase, we obtain for q_ν numbers between 4% and 6% and total energies $E_\nu \sim \langle L_\nu\rangle t_{acc}$ around 3×10^{52} ergs (Table 2). Annihilation of neutrino pairs, $\nu\bar{\nu} \to e^+e^-$, deposits energy at rates up to $\dot{E}_{\nu\bar{\nu}} \sim 2 \times 10^{52}$ ergs s^{-1} in the vicinity of the black hole (Fig. 4). This corresponds to total energies $E_{\nu\bar{\nu}} \sim \dot{E}_{\nu\bar{\nu}}t_{acc}$ as high as ~10^{51} ergs and annihilation efficiencies $q_{\nu\bar{\nu}} = E_{\nu\bar{\nu}}/\langle L_\nu\rangle$ of 1%–3%. These estimates should not change much if the different effects of general relativity on $\nu\bar{\nu}$ annihilation are taken into account in combination (Ruffert & Janka 1999; Asano & Fukuyama 1999), but general relativistic simulations of the merging are very important. More energy could be pumped into the $e^\pm\gamma$ fireball when the black hole rotates rapidly (Popham et al. 1999) or if magnetic fields are able to tap the rotational energy of the accretion torus and of the black hole with higher efficiency than $\nu\bar{\nu}$ annihilation does (Blandford & Znajek 1977). This seems to be necessary for the long and very energetic GRBs (Mészáros, Rees, & Wijers 1999; Brown et al. 1999; Lee, Wijers, & Brown 1999).

REFERENCES

Asano, K., & Fukuyama, T. 1999, ApJ, submitted
Bethe, H. A., & Brown, G. E. 1998, ApJ, 506, 780
———. 1999, ApJ, 517, 318
Bildsten, L., & Cutler, C. 1992, ApJ, 400, 175
Blanchet, L., Damour, T., & Schäfer, G. 1990, MNRAS, 242, 289
Blandford, R. D., & Znajek, R. L. 1977, MNRAS, 179, 433
Blinnikov, S. I., Novikov, I. D., Perevodchikova, T. V., & Polnarev, A. G. 1984, Soviet Astron. Lett., 10, 177
Brown, G. E., Wijers, R. A. M. J., Lee, C.-H., Lee, H. K., & Bethe, H. A. 1999, ApJ, submitted (astro-ph/9905337)
Eberl, T. 1998, M.S. thesis, Tech. Univ. Munich
Eichler, D., Livio, M., Piran, T., & Schramm, D. N. 1989, Nature, 340, 126
Fryer, C., Woosley, S. E., & Hartmann D. H. 1999, ApJ, submitted (astro-ph/9904122)
Fryer, C., Woosley, S. E., Herant, M., & Davies, M. B. 1999, ApJ, 520, 650
Kluźniak, W., & Lee, W. H. 1998, ApJ, 494, L53
Lai, D., Rasio, F. A., & Shapiro, S. L. 1994, ApJ, 423, 344
Lattimer, J. M., & Schramm, D. N. 1974, ApJ, 192, L145
Lattimer, J. M., & Swesty, F. D. 1991, Nucl. Phys. A, 535, 331

Lee, W. H., Kluźniak, W. 1998, ApJ, submitted (astro-ph/9808185)
———. 1999, MNRAS, 308, 780
Lee, H. K., Wijers, R. A. M. J., & Brown, G. E. 1999, Phys. Rep., submitted (astro-ph/9906213)
Mao, S., Narayan, R., & Piran, T. 1994, ApJ, 420, 171
Mészáros, P. 1999, in Proc. 19th Texas Symp. on Relative Astrophysics and Cosmology (Amsterdam: Elsevier), in press (astro-ph/9904038)
Mészáros, P., Rees, M. J., & Wijers, R. A. M. J. 1999, NewA, 4, 303
Narayan, R., Piran, T., & Shemi, A. 1991, ApJ, 379, L17
Paczyński, B. 1991, Acta Astron., 41, 257
Podsiadlowski, Ph., Joss, P. C., & Hsu, J. J. L. 1992, ApJ, 391, 246
Popham, R., Woosley, S. E., & Fryer, C. 1999, ApJ, 518, 356
Portegies Zwart, S. F. 1998, ApJ, 503, L53
Rasio, F. A., & Shapiro, S. L. 1994, ApJ, 432, 242
Ruffert, M., & Janka, H.-Th. 1999, A&A, 344, 573
Ruffert, M., Janka, H.-Th., & Schäfer, G. 1996, A&A, 311, 532
Ruffert, M., Janka, H.-Th., Takahashi, K., & Schäfer, G. 1997, A&A, 319, 122
Uryū, K., & Eriguchi, Y. 1999, MNRAS, 303, 329